Glutathione Deficiency of the Arabidopsis Mutant *pad2-1* Affects Oxidative Stress-Related Events, Defense Gene Expression, and the Hypersensitive Response[1][C][W][OA]

Carole Dubreuil-Maurizi[2], Jan Vitecek, Laurent Marty, Lorelise Branciard, Patrick Frettinger, David Wendehenne, Andreas J. Meyer[2], Felix Mauch, and Benoît Poinssot*

Université de Bourgogne, UMR Plante Microbe Environnement, INRA UMR 1088, CNRS UMR 5184, F–21000 Dijon, France (C.D.-M., J.V., P.F., D.W., B.P.); Institute of Biophysics, Academy of Sciences of the Czech Republic, CZ–61265 Brno, Czech Republic (J.V.); Heidelberg Institute for Plant Science, Heidelberg University, D–69120 Heidelberg, Germany (L.M., A.J.M.); and Department of Biology, University of Fribourg, CH–1700 Fribourg, Switzerland (L.B., F.M.)

The Arabidopsis (*Arabidopsis thaliana*) phytoalexin-deficient mutant *pad2-1* displays enhanced susceptibility to a broad range of pathogens and herbivorous insects that correlates with deficiencies in the production of camalexin, indole glucosinolates, and salicylic acid (SA). The *pad2-1* mutation is localized in the *GLUTAMATE-CYSTEINE LIGASE* (*GCL*) gene encoding the first enzyme of glutathione biosynthesis. While *pad2-1* glutathione deficiency is not caused by a decrease in *GCL* transcripts, analysis of GCL protein level revealed that *pad2-1* plants contained only 48% of the wild-type protein amount. In contrast to the wild type, the oxidized form of GCL was dominant in *pad2-1*, suggesting a distinct redox environment. This finding was corroborated by the expression of GRX1-roGFP2, showing that the cytosolic glutathione redox potential was significantly less negative in *pad2-1*. Analysis of oxidative stress-related gene expression showed a higher transcript accumulation in *pad2-1* of *GLUTATHIONE REDUCTASE*, *GLUTATHIONE-S-TRANSFERASE*, and *RESPIRATORY BURST OXIDASE HOMOLOG D* in response to the oomycete *Phytophthora brassicae*. Interestingly, oligogalacturonide elicitation in *pad2-1* revealed a lower plasma membrane depolarization that was found to act upstream of an impaired hydrogen peroxide production. This impaired hydrogen peroxide production was also observed during pathogen infection and correlated with a reduced hypersensitive response in *pad2-1*. In addition, a lack of pathogen-triggered expression of the *ISOCHORISMATE SYNTHASE1* gene, coding for the SA-biosynthetic enzyme isochorismate synthase, was identified as the cause of the SA deficiency in *pad2-1*. Together, our results indicate that the *pad2-1* mutation is related to a decrease in GCL protein and that the resulting glutathione deficiency negatively affects important processes of disease resistance.

Interactions between plants and microbes are the result of a finely tuned coevolution. To counter microbial attacks, plants have developed perception systems that activate various defense mechanisms. Two main defense pathways are described in plant innate immunity (Boller and Felix, 2009). The first, named pathogen-associated molecular pattern (PAMP)-triggered immunity, is based on the recognition of pathogen-, microbe-, or damage-associated molecular patterns by pattern recognition receptors (Jones and Dangl, 2006). The second and more specialized effector-triggered immunity is activated when plant disease resistance gene products detect the presence of pathogen effectors.

The perception of an invader's molecular tag is followed by several changes in plants (Tsuda and Katagiri, 2010). At the cellular level, many signaling events are rapidly detected, such as ion fluxes (Ca^{2+}, K^+, NO_3^-, Cl^-) and enhanced production of reactive oxygen species (ROS), mainly catalyzed by plasma membrane NADPH oxidases, encoded by *Respiratory Burst Oxidase Homolog* (*Rboh*) genes (Simon-Plas et al., 2002; Torres et al., 2002, 2006). This oxidative burst contributes, together with nitric oxide (NO) production, redox state changes, and mitogen-activated protein kinase cascade activation, to a transcriptional

[1] This work was supported by a grant from the French Ministère de l'Enseignement Supérieur et de la Recherche to C.D.-M., by the Conseil Régional de Bourgogne, Bureau Interprofessionnel des Vins de Bourgogne, by the Agence Nationale de la Recherche Genoplante (grant no. GENO-148G), and by the Comité National des Interprofessions des Vins d'Appellation d'Origine.

[2] Present address: Institute of Crop Science and Resource Conservation, Chemical Signaling, University of Bonn, Friedrich-Ebert-Allee 144, D–53113 Bonn, Germany.

* Corresponding author; e-mail benoit.poinssot@dijon.inra.fr.

The author responsible for distribution of materials integral to the findings presented in this article in accordance with the policy described in the Instructions for Authors (www.plantphysiol.org) is: Benoît Poinssot (benoit.poinssot@dijon.inra.fr).

[C] Some figures in this article are displayed in color online but in black and white in the print edition.

[W] The online version of this article contains Web-only data.

[OA] Open Access articles can be viewed online without a subscription.

www.plantphysiol.org/cgi/doi/10.1104/pp.111.182667

reprogramming leading to the activation of defense responses (Asai et al., 2002; Wendehenne et al., 2002; Torres et al., 2006; Besson-Bard et al., 2008; Foyer et al., 2009). Changes in hormonal balance, particularly salicylic acid (SA), jasmonic acid (JA), and ethylene (ET), have been shown to be key events in the activation and fine-tuning of plant immunity upon pathogen attack. Finally, the production of antimicrobial compounds such as phytoalexins (Hammerschmidt, 1999), pathogenesis-related (PR) proteins (van Loon et al., 2006), and cell wall strengthening arise from this defense activation to restrict pathogen growth.

In Arabidopsis (*Arabidopsis thaliana*), it is now well accepted that SA signaling is generally important for immunity against biotrophs, whereas JA/ET signaling is important for immunity against necrotrophs (Glazebrook, 2005). However, it has been shown that disease resistance of Arabidopsis against the oomycete pathogen *Phytophthora brassicae* is SA, JA, and ET independent but needs the indole glucosinolate/camalexin pathways (Roetschi et al., 2001; Schlaeppi et al., 2010). In the case of biotrophic pathogens, like *P. brassicae*, a form of plant programmed cell death, named the hypersensitive response (HR), can be detected during the incompatible interaction that may restrict pathogen growth (Roetschi et al., 2001; Hofius et al., 2007). On the whole, this complex defense network allows plants to resist most of their invaders.

Studies with plant mutants have provided essential information to understand the molecular mechanisms underlying plant disease resistance. The Arabidopsis phytoalexin-deficient mutant *pad2-1* displays susceptibility to a broad range of pathogens and pests, including necrotrophs (*Botrytis cinerea*, *Alternaria brassicicola*), hemibiotrophs and biotrophs (*P. brassicae*, *Pseudomonas syringae*), and insect herbivores (*Spodoptera littoralis*; Glazebrook and Ausubel, 1994; Glazebrook et al., 1997; Reuber et al., 1998; Roetschi et al., 2001; Ferrari et al., 2003; van Wees et al., 2003; Bohman et al., 2004; Parisy et al., 2007; Schlaeppi et al., 2008). The *pad2-1* mutation is localized in the single-copy gene At4g23100, which encodes Glutamate-Cysteine Ligase (GCL), the first enzyme involved in the biosynthesis of the tripeptide glutathione. Due to mutation S298N in GCL, *pad2-1* contains only approximately 20% of wild-type glutathione (Parisy et al., 2007). Three other allelic mutations have been found in GCL: the *root-meristemless1* mutant (*rml1*; D258N) possesses only approximately 3% of wild-type glutathione, which leads to the frequent abortion of plant development (Vernoux et al., 2000); the *cadmium-sensitive2-1* mutant (*cad2-1*; ΔP237, ΔK238, and V239L) has approximately 30% of wild-type glutathione and is sensitive to heavy metals (Cobbett et al., 1998) but is moderately susceptible to *P. brassicae* (Parisy et al., 2007); the *regulator of APX2 1-1* mutant (*rax1-1*; R228K) has approximately 40% of wild-type glutathione and is sensitive to high light (Ball et al., 2004) but shows a wild-type resistance to *P. brassicae* (Parisy et al., 2007). Thus, these results highlighted that glutathione plays a major role in many cellular processes such as development and responses to biotic and abiotic stresses (Potters et al., 2002; Noctor, 2006; Foyer and Noctor, 2011). Complementary results have shown that glutathione biosynthesis is controlled by transcriptional and post-translational regulation of GCL and not by its second step catalyzed by glutathione synthase (GS; May et al., 1998; Jez et al., 2004; Hicks et al., 2007).

Many studies have shown that *pad2-1* displays a pleiotropic phenotype. Concerning defense responses, the production of camalexin, the main phytoalexin of Arabidopsis, is strongly affected in *pad2-1* in response to *P. syringae* pv *maculicola* (approximately 15% of the wild type; Glazebrook and Ausubel, 1994), *B. cinerea* (approximately 25% of the wild type; Ferrari et al., 2003), *A. brassicicola* (approximately 35% of the wild type; van Wees et al., 2003), or *P. brassicae* (approximately 40% of the wild type; Roetschi et al., 2001; Parisy et al., 2007). This camalexin deficiency is directly due to glutathione depletion, since glutathione is required for glutathione *S*-transferase (GSTF6)-catalyzed synthesis of glutathione-indole-3-acetonitrile, a precursor of camalexin biosynthesis (Su et al., 2011). Besides, the impaired camalexin biosynthesis and resistance to *P. brassicae* in *pad2-1* can be restored using either glutathione feeding or transformation with wild-type *GCL* cDNA (Parisy et al., 2007).

Glucosinolates are another class of sulfur-containing compounds of Brassicaceae whose degradation products are well known to be toxic against insects and pathogens (Halkier and Gershenzon, 2006). Interestingly, Schlaeppi and colleagues recently showed that *pad2-1* is impaired in the production of indole glucosinolates in response to insects (approximately 55% of the wild type; Schlaeppi et al., 2008) or *P. brassicae* infection (approximately 40% of the wild type; Schlaeppi et al., 2010). Moreover, stress-induced SA accumulation and *PR-1* expression are also very low in *pad2-1* in response to *P. brassicae* (Roetschi et al., 2001). The SA deficiency of *pad2-1* is possibly linked to the requirement of glutathione to modulate the redox state needed for the oligomer/monomer transition of *Nonexpressor of Pathogenesis-Related1* (*NPR1*) genes preceding NPR1 translocation into the nucleus to activate *PR-1* gene expression (Després et al., 2003; Mou et al., 2003; Pieterse and Van Loon, 2004). However, it remains unexplained how glutathione modulates SA acting upstream of NPR1.

Many studies reported that the total glutathione concentration, as well as the ratio of reduced to oxidized forms of glutathione, affect cellular redox homeostasis during plant development or environmental stress (May et al., 1998; Mullineaux and Rausch, 2005; Foyer and Noctor, 2011). These cellular redox changes influence the genome-wide expression profile (Ball et al., 2004) and protein activity. For example, GCL is redox activated by the formation of two disulfide bonds (Jez et al., 2004; Hothorn et al., 2006; Hicks et al., 2007). Despite the apparent impact of glutathione depletion on defense signaling events and responses

such as HR, these underlying mechanisms have not yet been studied using a genetic approach.

The aim of this study was to identify the molecular origin of the glutathione depletion in *pad2-1* and to investigate the putative links between glutathione, the cellular redox potential, ROS production, defense gene expression, and HR. For this purpose and to better understand the disease susceptibility of *pad2-1*, we compared early signaling events occurring in wild-type Columbia-0 (Col-0) and *pad2-1* cells treated with oligogalacturonides (OG), a damage-associated molecular pattern that elicits typical defense responses, and during plant infection with *P. brassicae*. Our results indicate that the glutathione deficiency in *pad2-1* is related to a decreased GCL protein content. They also highlight a role of glutathione in modulating the cellular redox environment, membrane depolarization, ROS and NO production, expression of key defense-related genes, and HR development. These data highlight the crucial role of glutathione in signaling processes underlying essential defense responses in plants.

RESULTS

The GCL Protein Amount Is Lower in *pad2-1* and Its Redox State Is More Oxidized

The *pad2-1* mutation S298N of GCL causes a low glutathione content as compared with the wild type (approximately 20% of the wild type; Parisy et al., 2007). Since the glutathione deficiency of *pad2-1* is not related to a reduced expression of *GCL* or *GS* genes, which encode the two enzymes involved in glutathione synthesis (Parisy et al., 2007), we analyzed if the S298N mutation affects the GCL protein amount. While the *cad2-1*, *rax1-1*, and *rml1-1* mutations have been proposed to directly affect amino acid residues involved in the binding of one of the GCL substrates (Glu, Cys, or ATP; Hothorn et al., 2006), nothing was known about the *pad2-1* mutation. Using PyMOL software (PyMOL Molecular Graphics System; Schrödinger), in silico prediction indicated that the S298N exchange in *pad2-1* did not affect the ternary structure of GCL, contrary to *cad2-1* and *rax1-1* mutations, which displayed a minor structure modification in one β-sheet (data not shown). Moreover Ser-298 has not been described to be involved in the catalytic site of GCL (involving 12 residues in Arabidopsis: Glu-115, Arg-228, Tyr-229, Met-232, Met-247, Thr-250, Asp-258, Arg-300, Trp-304, Tyr-338, Phe-383, and Tyr-391) or in its thiol-based redox regulation sites (Hothorn et al., 2006; Hicks et al., 2007; Gromes et al., 2008). To test the hypothesis that the *pad2-1* mutation could affect GCL protein folding or stability, we first compared the GCL protein level between *pad2-1* and wild-type plants by western-blot analysis using an antibody raised against purified recombinant AtGCL (Hicks et al., 2007). As GCL occurs in oxidized and reduced forms, tissue extracts were reduced prior to western blotting. Interestingly, *pad2-1* leaf tissue contained only 48% of the wild-type amount of GCL. However, in the allelic *cad2-1* and *rax1-1* mutants, the GCL levels were almost the same as in the wild type (Fig. 1A). These results show that *pad2-1* is the only one to display a very low GCL protein level, which could explain its low glutathione content.

GCL activity is regulated by cellular redox state (Jez et al., 2004; Hothorn et al., 2006; Hicks et al., 2007). In Arabidopsis, the oxidation of the inactive reduced form switches the protein into an active form via the formation of intramolecular disulfide bonds (Hicks et al., 2007). Therefore, we investigated the oxidized and reduced forms of GCL after oxidative stress (Fig. 1B). For this purpose, leaf discs were treated with 5 mM hydrogen peroxide (H_2O_2) and total proteins were extracted in reducing (+dithiothreitol [DTT]) or nonreducing (−DTT) conditions and examined by western blotting. Under reducing conditions, only one band was detected, with a molecular mass of 50 kD in both wild-type and *pad2-1* plants (Fig. 1). In nonreducing conditions, two bands were detected in wild-type plants, corresponding to the oxidized and

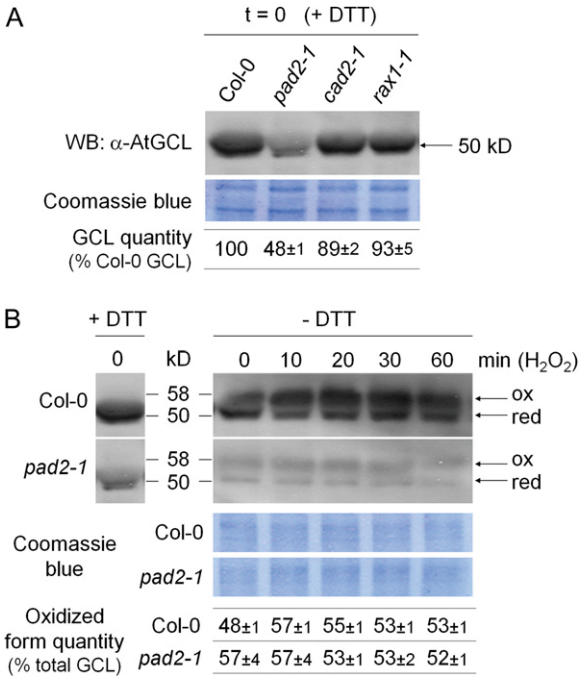

Figure 1. Analysis of the total content and redox state of GCL. Total proteins were extracted under reducing (+0.1 M DTT) or nonreducing (−DTT) conditions. Oxidized (ox) and reduced (red) forms of GCL were analyzed by western blotting (WB) using an antibody raised against recombinant AtGCL. A, Total amount of GCL in Col-0 and glutathione-deficient mutants *pad2-1*, *cad2-1*, and *rax1-1*. B, Changes of the redox state of GCL after H_2O_2 treatment in Col-0 and *pad2-1* plants. Leaf discs were treated with 5 mM H_2O_2. Results are representative of three independent experiments. Equal protein loading was checked by staining with Coomassie blue. The percentage values for total GCL are means ± SE of three independent experiments. [See online article for color version of this figure.]

reduced forms of GCL, with apparent molecular masses of 56 and 50 kD, respectively. In accordance with Hicks et al. (2007), the reduced form was found to be dominant in wild-type plants. Oxidative stress induced by H_2O_2 shifted GCL to the oxidized active form. Under nonreducing conditions, both the reduced and oxidized forms of GCL were detected at a very low level in *pad2-1*. However, in contrast to wild-type plants, the oxidized form of GCL was already dominant at 0 min, and no obvious change of the redox state of the enzyme was observed within 60 min after treatment with H_2O_2. Thus, the redox regulation of the GCL enzyme is impaired in *pad2-1* plants. These data also suggest that *pad2-1* might display a distinct redox environment, known to be essentially maintained by the glutathione pool (Foyer and Noctor, 2011).

The Glutathione Redox Potential Is Less Reducing in *pad2-1* Than in the Wild Type

To investigate whether the cytosolic glutathione redox potential (E_{GSH}) differs between *pad2-1* and the wild type, E_{GSH} was measured with the glutathione-specific redox-sensitive GFP (roGFP) variant GRX1-roGFP2. It was previously demonstrated that this fusion sensor of the human Glutaredoxin1 (GRX1) and roGFP2 equilibrates with glutathione and thus reports the local E_{GSH} (Gutscher et al., 2008).

Wild-type and *pad2-1* seedlings expressing GRX1-roGFP2 in the cytosol were subjected to ratiometric analysis of GRX1-roGFP2 fluorescence through confocal imaging with excitation at 405 and 488 nm (Fig. 2). In basal conditions, the 405/488 fluorescence ratio of GRX1-roGFP2 was higher in *pad2-1* (2.03 ± 0.36) than in the wild type (0.51 ± 0.14), indicating that GRX1-roGFP2 is more oxidized in *pad2-1* plants (Fig. 2).

For probe calibration, wild-type and *pad2-1* tissues were treated with 10 mM H_2O_2 or 10 mM DTT to fully oxidize or reduce the GRX1-roGFP2 protein (Fig. 2B). After 10 mM H_2O_2 treatment, the GRX1-roGFP2 ratio of the wild type (4.52 ± 1.41) and *pad2-1* (4.24 ± 1.46) increased to almost the same value. Similarly, the ratio of the DTT-treated tissues was comparable in the wild type (0.46 ± 0.06) and *pad2-1* (0.61 ± 0.13). These results showed that the ratiometric behavior of the fluorescent probe, including its dynamic range, was the same in the mutant and the wild-type plants. Based on these calibration values, the ratio values measured in leaves under nonstress conditions were converted to E_{GSH} according to Meyer et al. (2007). While E_{GSH} was −312 ± 10 mV in the wild type, it was only −275 ± 5 mV in *pad2-1*. Together, these data indicated that the glutathione redox buffer in *pad2-1* has less reducing power than that in the wild type.

Expression of Oxidative Stress-Related Genes Is Higher in *pad2-1* during *P. brassicae* Infection

Since E_{GSH} is less reducing in *pad2-1* compared with the wild type, we evaluated whether *pad2-1* perceived

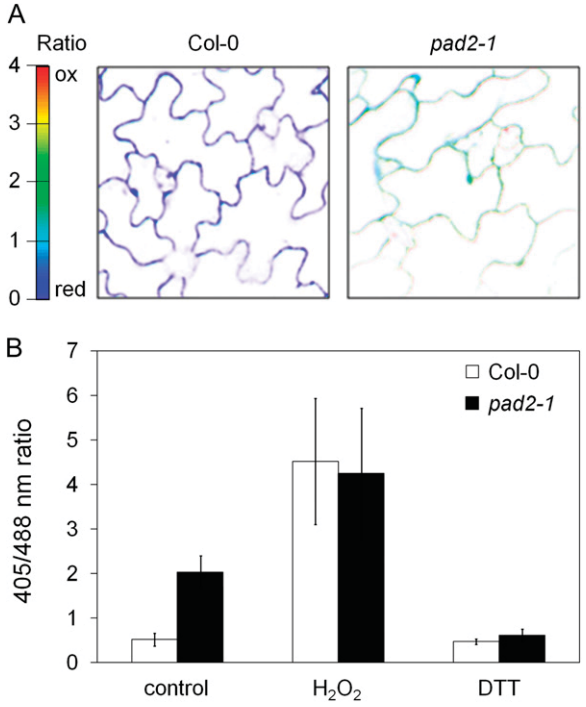

Figure 2. Comparison of the glutathione redox potential of Col-0 and *pad2-1* epidermal cells expressing GRX1-roGFP2 in the cytosol. A, Images were taken by confocal laser scanning microscopy. GRX1-roGFP2 was excited with 405- and 488-nm wavelengths. The color scale of the fluorescence ratio represents the redox state of roGFP2 oscillating between an oxidized (ox) state (red) and a reduced (red) state (blue). B, Quantitative ratio values for images taken on Col-0 and *pad2-1* mutant tissue. Water-treated (control), fully oxidized (10 mM H_2O_2), or fully reduced (10 mM DTT) samples for Col-0 and the *pad2-1* mutant were compared (mean ± SE; $n = 6$). Results are representative of three independent experiments.

a stronger oxidative stress during pathogen infection. Thus, we chose to analyze the expression of oxidative stress-related genes by real-time quantitative PCR at 24 h post inoculation (hpi) with *P. brassicae* (Fig. 3).

NADPH-dependent Glutathione Reductase1 (GR1) is involved in the glutathione-ascorbate cycle by catalyzing the regeneration of oxidized to reduced glutathione under oxidative stress (Foyer and Noctor, 2011). Indeed, the *gr1* mutant of Arabidopsis showed a low capacity to maintain a reduced glutathione pool after H_2O_2 treatment and displayed a similar E_{GSH} to *pad2-1* (Marty et al., 2009). During infection, *P. brassicae* triggered a significant expression of *GR1* transcripts that was more pronounced in *pad2-1* than in the wild type (Fig. 3). No significant difference was found between unchallenged *pad2-1* and wild-type plants.

Among plant *GST* genes, which are induced by a variety of stimuli, *AtGSTF6* (also called *AtGST1*) was reported to be induced upon infection or in response to H_2O_2 treatment (Marrs, 1996; Nutricati et al., 2006; Belhaj et al., 2009). In this study, we show that the transcript level of *GSTF6* was significantly up-regulated

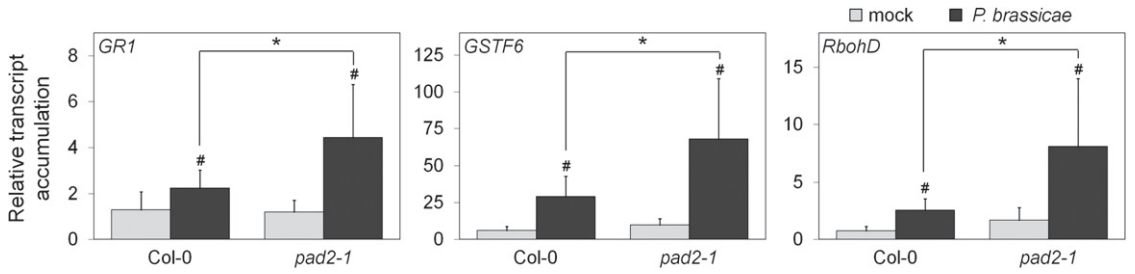

Figure 3. Expression of oxidative stress-related genes in response to *P. brassicae* at 24 hpi. Plant leaves were infected by agar plug inoculation of 8-d-old mycelium. Mycelium-free plugs were used for mock treatment. The transcript accumulation of genes encoding *GR1*, *GSTF6*, and *RbohD* was analyzed by real-time qPCR. After normalization with *UBQ10*, results were expressed as fold change in transcript level compared with the time zero sample (mean ± SE; $n = 3$) from three independent biological experiments. Hash marks indicate statistically significant differences between mock and infected samples ($P < 0.05$), and asterisks indicate statistically significant differences between infected Col-0 and infected *pad2-1* samples ($P < 0.05$), using unpaired heteroscedastic Student's *t* test.

in response to *P. brassicae* both in *pad2-1* and the wild type (Fig. 3). However, the increase in transcript accumulation in *pad2-1* was more than 2-fold higher than in the wild type.

In addition to *GR1* and *GSTF6* genes, we chose to analyze the expression of the *RbohD* gene, because *Rboh* genes encode NADPH oxidase enzymes that catalyze the production of the ROS $O_2^{\cdot -}$ (Levine et al., 1994; Torres et al., 2002; Sagi and Fluhr, 2006). Moreover, *RbohD* has been shown to be involved in the enhanced production of H_2O_2 detected after OG elicitation (Galletti et al., 2008) or in response to *P. brassicae* (Belhaj et al., 2009). Figure 3 shows that the transcript level of the *RbohD* gene was 2.5 times higher in *pad2-1* compared with wild-type plants in response to *P. brassicae*.

pad2-1 Is Impaired in H_2O_2 and NO Production during Biotic Stresses

As the expression of the oxidative stress-related marker genes *GR1*, *GSTF6*, and *RbohD* was significantly higher in *pad2-1* than in the wild type, we checked H_2O_2 production in response to two biotic stress conditions: elicitation by OG and inoculation with *P. brassicae* (Fig. 4).

H_2O_2 production was first determined in cell suspensions using the chemiluminescence of luminol. In wild-type cells, OG treatment elicited a transient increase in H_2O_2 accumulation, which peaked at 10 min and decreased slowly until 120 min (Fig. 4A). In *pad2-1* cells, the transient increase in H_2O_2 production was delayed and represented only 30% of the maximal production detected in wild-type cells. This low content of H_2O_2 in *pad2-1* was due to an impairment of its production rather than to an increase in its degradation, as H_2O_2 half-life and global peroxidase or catalase activities were similar in the two genotypes (Supplemental Fig. S1).

The unexpected loss of OG-induced H_2O_2 accumulation was also observed in *pad2-1* leaves using a modified diaminobenzidine (DAB) staining method (Fig. 4B). In presence of peroxidases, which are ubiquitous in plant tissue, H_2O_2 reacts with DAB to produce brown precipitates (Thordal-Christensen et al., 1997). In order to allow a higher sensitivity of the approach, an excess of horseradish peroxidase was added to the DAB solution prior to infiltration into

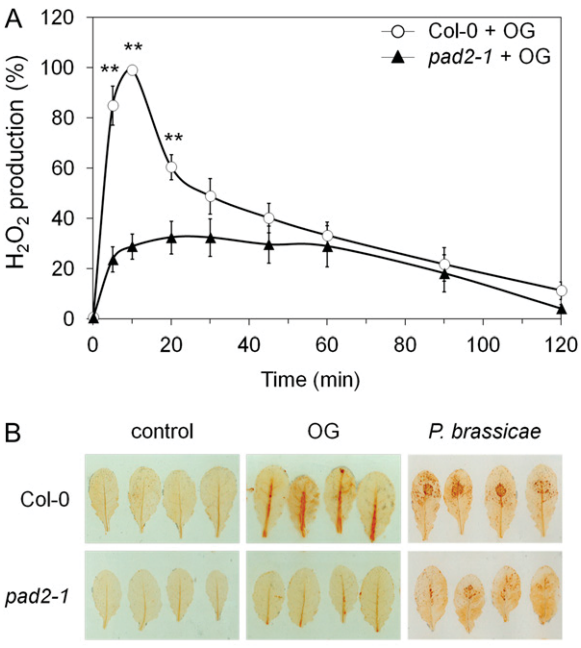

Figure 4. H_2O_2 production in response to OG or *P. brassicae* in Col-0 and *pad2-1*. A, H_2O_2 was measured using the chemiluminescence of luminol after OG treatment (0.5 g L^{-1}) in Col-0 and *pad2-1* cell suspensions. Data are expressed as percentage of the maximum H_2O_2 production in OG-treated Col-0 cells. Values are means ± SE of three independent experiments. Asterisks indicate statistically significant differences between the wild type and *pad2-1*, using Student's *t* test ($P < 0.01$). B, In planta H_2O_2 detection. Leaves were treated with 2.5 g L^{-1} OG during 20 min or inoculated for 1 d with *P. brassicae* agar plugs before DAB staining. H_2O_2 production was detected as brown precipitates. Results are representative of three independent experiments.

leaves. This modification allowed improved visualization of OG-induced H_2O_2 accumulation. No precipitate was detected in control leaves of wild-type and *pad2-1* plants. While a strong brown precipitate was observed in wild-type leaves treated during 20 min with OG, H_2O_2 production was only weakly detected in *pad2-1* leaves under the same conditions. Similar results were obtained with leaves infected with *P. brassicae* for 1 d. Wild-type leaves showed an intense brown precipitate at the infection site, whereas the response was much weaker in *pad2-1* leaves (Fig. 4B). H_2O_2 accumulation in response to OG treatment or *P. brassicae* infection was completely abolished in the *rbohD* mutant (data not shown; Belhaj et al., 2009), demonstrating that the H_2O_2 accumulation in response to *P. brassicae* or OG treatment depends on RbohD.

Another second messenger rapidly produced after elicitation is NO (Foissner et al., 2000; Besson-Bard et al., 2008). Using the NO-sensitive probe 4,5-diaminofluorescein diacetate (DAF-2DA), intracellular NO production was monitored during 12 h in leaf discs infiltrated with OG (8-h data shown in Supplemental Fig. S2). In water-infiltrated leaf discs, a basal fluorescence was observed in the wild type and *pad2-1*, probably reflecting constitutive NO production and/or the wounding response caused by the preparation of leaf discs. After OG treatment, an increase in fluorescence was observed in the wild type and *pad2-1*. However, this increase was significantly less pronounced in *pad2-1* at 8 h after treatment. The use of the specific NO scavenger carboxy-PTIO confirmed the NO specificity of the probe by suppressing the fluorescence triggered by OG in wild-type and *pad2-1* cells.

The Lower Plasma Membrane Depolarization in *pad2-1* Cells Acts Upstream of ROS Production

Ion fluxes have been described to act upstream of the oxidative burst, known to be involved in HR and notably observed during the resistance of wild-type Arabidopsis to *P. brassicae* (Heath, 2000; Delledonne et al., 2001; Roetschi et al., 2001; Wendehenne et al., 2002; Greenberg and Yao, 2004). Having established that the production of H_2O_2 was altered in *pad2-1*, we checked whether a perturbation of ion fluxes at the plasma membrane level could be the source of this impairment in *pad2-1*. To test the hypothesis, wild-type and *pad2-1* cell suspensions were treated with OG and changes in the plasma membrane potential were monitored by using the voltage-sensitive fluorescent probe bis-(1,3-dibutylbarbituric acid)-trimethine oxonol [$DiBAC_4(3)$; Fig. 5; Lamotte et al., 2006; Konrad and Hedrich, 2008].

In wild-type and *pad2-1* cells responding to OG treatment, a transient increase in fluorescence, reflecting a plasma membrane depolarization, occurred within the first 5 min and then peaked at 10 min. Within 30 min, $DiBAC_4(3)$ fluorescence returned to the basal level (Fig. 5). Interestingly, in *pad2-1* cells, the maximal fluorescence at 10 min was two times lower than in wild-type cells. This result shows that *pad2-1* is partly impaired in OG-dependent plasma membrane depolarization. Addition of the anionic channel inhibitor niflumic acid to wild-type cells 10 min before treatment totally inhibited the increase in $DiBAC_4(3)$ fluorescence, indicating the involvement of anion channels in this process (Supplemental Fig. S3A). Moreover, the total inhibition of OG-dependent H_2O_2 production by niflumic acid treatment provided evidence that ROS production occurs downstream of anion channel activation and plasma membrane depolarization (Supplemental Fig. S3B).

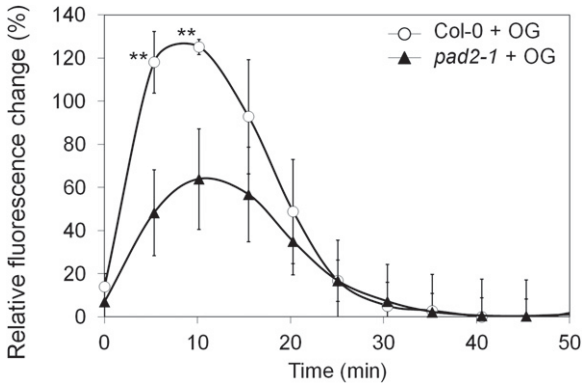

Figure 5. Plasma membrane potential changes in response to OG treatment in Col-0 and *pad2-1* cell suspensions. Cells were incubated with the voltage-sensitive fluorescent probe $DiBAC_4(3)$ (10 μM) in the dark before OG treatment (0.5 g L^{-1}). Plasma membrane depolarization was monitored by following the variation of $DiBAC_4(3)$ fluorescence and was expressed as a relative percentage: [fluorescence (OG) – fluorescence (water)]/fluorescence (water). The chart shows mean values ± SE out of five independent experiments. Asterisks indicate statistically significant differences between the wild type and *pad2-1*, using Student's *t* test ($P < 0.01$).

These results indicate that *pad2-1* is impaired in plasma membrane depolarization and H_2O_2 and NO production during elicitation.

pad2-1 Is Impaired in HR Development in Response to *P. brassicae*

In many plant-pathogen interactions, one of the mechanisms stopping the pathogen invasion into leaf tissue is the HR. Since *pad2-1* is impaired in key defense-related signaling events in response to biotic stresses and because it is susceptible to many pathogens, we compared HR formation in the wild type and *pad2-1* after inoculation with *P. brassicae* (Fig. 6). Plants were inoculated by spraying a zoospore suspension, and the formation of HR and pathogen growth were analyzed by trypan blue staining at 1 d post inoculation (dpi). No significant difference in zoospore germination and pathogen penetration efficiency was found between the wild type and *pad2-1* (data not shown). However, in wild-type plants, HR occurred in 86% of attempted infections, whereas this percentage

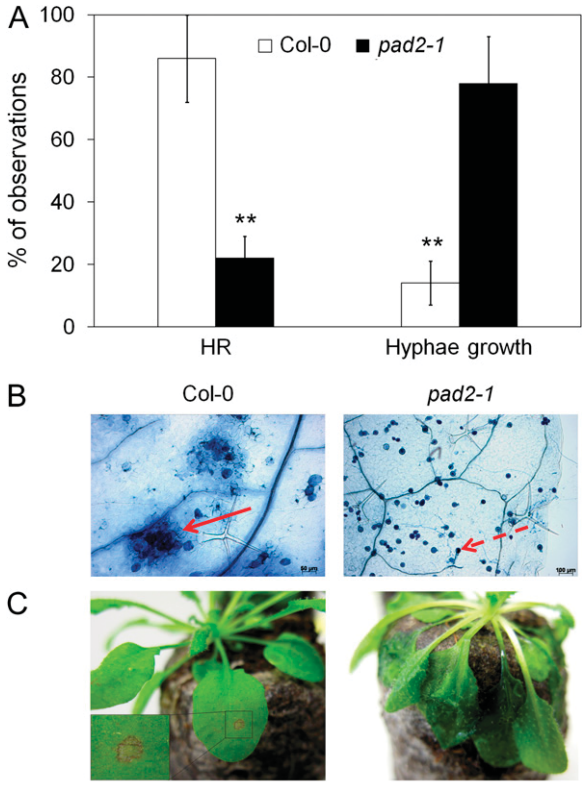

Figure 6. HR and *P. brassicae* development in Col-0 and *pad2-1* plants. Leaves were inoculated by spraying a zoospore suspension of *P. brassicae* (10^5 zoospores mL^{-1}) and harvested at the time indicated below. HR and pathogen structures were observed with lactophenol trypan blue staining. A, Percentages of the microscopic observations of three biological replicates at 1 dpi. Asterisks indicate statistically significant differences between the wild type and *pad2-1*, using a χ^2 test ($P < 0.01$). B, Microscopic observation of HR (arrow) and pathogen development (dotted arrow; oospore) at 7 dpi. C, HR and water-soaked disease symptoms at 7 dpi with *P. brassicae* agar plugs in Col-0 and *pad2-1* plants, respectively.

was reduced to 22% in *pad2-1* (Fig. 6A). The reduced rate of HR formation correlated with the enhanced rate of pathogen growth. Encysted zoospores producing hyphae were seen only in 14% of the observations in the wild type compared with 78% in *pad2-1* (Fig. 6A). The different responses of the two genotypes to *P. brassicae* were also illustrated at 7 dpi. The wild type showed HR at both microscopic and macroscopic levels (Fig. 6, B and C), whereas in *pad2-1*, the pathogen developed extensively, as demonstrated by the massive occurrence of oospores (Fig. 6B) and the wilting of leaves (Fig. 6C).

Expression of SA-Related Genes Is Impaired during *P. brassicae* Infection of *pad2-1*

One important phenotypic aspect observed in *pad2-1* is the impairment of SA accumulation in response to *P. brassicae* (Roetschi et al., 2001). In order to find the putative origin of this SA deregulation, we first analyzed the expression of the *ISOCHORISMATE SYNTHASE1* (*ICS1*) gene, which encodes an important enzyme involved in SA biosynthesis (Nawrath and Métraux, 1999; Wildermuth et al., 2001). *ICS1* transcript accumulation was 6-fold increased in the wild type in response to *P. brassicae*, but no increase in transcript level was detected in *pad2-1* (Fig. 7). In parallel, the regulation of *PR-1* and *NPR1* gene expression was checked at 24 hpi with *P. brassicae* (Fig. 7). In accordance with the low *ICS1* transcript levels and the previously reported reduction of SA accumulation in *pad2-1*, transcript accumulation of the SA marker gene *PR-1* was three times lower in *pad2-1* compared with the wild type. *NPR1* gene expression was not induced in either genotype.

Transcript Levels of Genes Involved in Camalexin and Indole Glucosinolate Biosynthesis Are Similar in *pad2-1* and the Wild Type

Together with camalexin, glucosinolates have recently been shown to play a major role in the resistance to *P. brassicae* (Schlaeppi et al., 2010). The *pad2-1* mutant displayed a reduced accumulation of camalexin and glucosinolates (Roetschi et al., 2001; Parisy et al., 2007; Schlaeppi et al., 2010). To understand whether this defense pathway was down-regulated at the transcriptional level, gene expression was analyzed for *CYP79B2* and *CYP79B3*, which encode two enzymes involved in the conversion of Trp to indole-3-aldoxime, a common precursor of camalexin and indole glucosinolates (Zhao et al., 2002; Bednarek et al., 2009). Furthermore, the expression of the indole glucosinolate-specific *CYP81F2* gene and the camalexin-specific *PAD3* gene (*CYP71B15*) were analyzed (Böttcher et al., 2009; Pfalz et al., 2009). All four genes were similarly up-regulated in response to *P. brassicae* in *pad2-1* and wild-type plants (Supplemental Fig. S4). Together, these results indicate that the impairment in the indole glucosinolate/camalexin pathway, revealed by the lower metabolite content in *pad2-1*, is not due to the different transcript accumulation of the analyzed biosynthetic genes.

DISCUSSION

The Glutathione Depletion in *pad2-1* Is Related to a Lower Amount of GCL Protein

GCL is described as the major control point of glutathione synthesis in plants, and the amount of glutathione seems to depend on the regulation of GCL at both transcriptional and posttranslational levels (May et al., 1998; Jez et al., 2004; Hicks et al., 2007). Under normal physiological conditions, *GCL* and *GS* transcript levels are similar in *pad2-1* and wild-type plants (Parisy et al., 2007). Moreover, during infection with *P. brassicae*, *GCL* and *GS* transcript accumulation is higher in *pad2-1* as compared with the wild type,

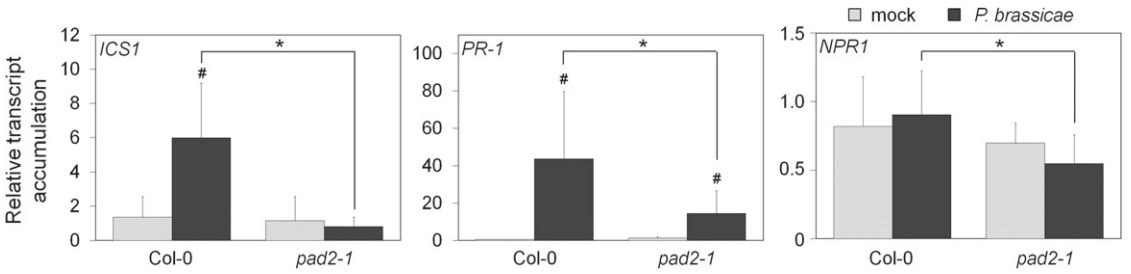

Figure 7. Expression of SA-related genes in response to *P. brassicae* at 24 hpi. Plant leaves were agar plug inoculated with 8-d-old mycelium. Mycelium-free plugs were used for mock treatment. The transcript accumulation of *ICS1*, *PR-1*, and *NPR1* was analyzed by real-time qPCR. After normalization with *UBQ10*, results were expressed as fold change in transcript level compared with the time zero sample (mean ± SE; $n = 3$) from three independent biological experiments. Hash marks indicate statistically significant differences between mock and infected samples ($P < 0.05$), and asterisks indicate statistically significant differences between infected Col-0 and infected *pad2-1* samples ($P < 0.05$), using unpaired heteroscedastic Student's *t* test.

while the glutathione level remains lower in the mutant (approximately 20% of the wild-type amount; Parisy et al., 2007).

To establish a functional relationship between glutathione and GCL in *pad2-1*, we compared the amount and posttranslational regulation of the GCL enzyme in *pad2-1* and wild-type plants. GCL activity is modulated by redox control through the formation of two intramolecular disulfide bonds (C186-C406 and C349-C364), which enable a switch of the inactive reduced form to the active oxidized one under oxidative conditions (Jez et al., 2004; Hothorn et al., 2006; Hicks et al., 2007). Under reducing conditions, our results showed that the total amount of GCL was drastically lower in *pad2-1* compared with the wild type or the two allelic mutants *cad2-1* and *rax1-1* (Fig. 1A). Studying the crystal structure of GCL, Hothorn et al. (2006) showed that *cad2-1* and *rax1-1* mutations are located in regions critical for binding of the substrates Glu and/or Cys, thus explaining the glutathione depletion in *cad2-1* and *rax1-1*. However, all the critical residues involved in the catalytic activity or the redox regulation of GCL are not affected by the *pad2-1* mutation S298N. Our results indicate that the glutathione deficiency of *pad2-1* is likely caused by a drastic decrease in GCL protein content. Nevertheless, we cannot fully exclude that the proximity of the *pad2-1* mutation to Arg-300 might affect Glu binding of the GCL enzyme (Hothorn et al., 2006), leading to a change in enzyme activity and thus a decrease in glutathione content.

pad2-1 Plants Sense a Permanent Oxidative Stress

Glutathione is known to play a central role in antioxidant processes as an efficient scavenger of ROS through its cysteinyl thiol group (Noctor, 2006), although its direct role is still disputed (Winterbourn, 2008). The balance between the reduced and oxidized forms of glutathione is involved in cellular redox homeostasis and influences, directly or indirectly, the regulation of many cellular processes at the gene and/or protein levels (Cobbett et al., 1998; Mou et al., 2003; Ball et al., 2004; Jez et al., 2004). To check whether the susceptibility of *pad2-1* to pathogens could be related to a deregulation of the glutathione-dependent control of the cellular redox state, we analyzed, on the one hand, the reduced and oxidized forms of GCL and, on the other hand, the E_{GSH} with the GRX1-roGFP2 fluorescent probe in vivo (Meyer et al., 2007; Gutscher et al., 2008; Schwarzländer et al., 2008).

Our study confirms that the oxidative stress triggered by H_2O_2 switches the reduced to the oxidized form of the GCL enzyme in the wild type (Fig. 1B), as demonstrated previously by Hicks et al. (2007). The more oxidized GCL protein observed in *pad2-1* (Fig. 1B) is most probably due to a less reducing E_{GSH} caused by the diminished glutathione levels in the mutant, as revealed by the GRX1-roGFP2 measurements.

In the absence of any treatment, GRX1-roGFP2 was more oxidized in *pad2-1* than in the wild type, indicating higher E_{GSH} in *pad2-1* (E_{GSH} of approximately −275 mV compared with −312 mV in the wild type). The *gr1* mutant of Arabidopsis showed a low capacity to maintain a reduced glutathione pool after H_2O_2 treatment and displayed a similar E_{GSH} to *pad2-1* (−270 mV; Marty et al., 2009). Similarly, in the glutathione-deficient *cad2-1* mutant, containing 30% of wild-type glutathione, an increased fraction of GRX1-roGFP2 is found in the oxidized state (E_{GSH} of approximately −300 mV; Meyer et al., 2007). The *gr1* and *cad2-1* mutants are susceptible to *P. syringae* pv *tomato* and pv *maculicola*, respectively (Parisy et al., 2007; Mhamdi et al., 2010). Moreover, *cad2-1* is moderately susceptible to *P. brassicae*, but not to such an extent as *pad2-1* (Parisy et al., 2007). All the above-mentioned mutants, having higher E_{GSH}, are more sensitive to pathogen attack (Meyer et al., 2007; Parisy et al., 2007; this work). These data collectively indicate that a shift in the E_{GSH} in the cytosol is sufficient to reduce plant disease resistance, as recently shown by Maughan et al. (2010). Modulation of the cellular redox state is known to be one of the components acting on the regulation of gene expression through

oxidation or a reduction of transcription factors (Apel and Hirt, 2004; Mittler et al., 2004). Interestingly, during *P. brassicae* infection, the expression of marker genes of oxidative stress, such as *GR1*, *GSTF6*, and *RbohD*, was significantly higher in *pad2-1*, suggesting the perception of a more oxidized environment during biotic stresses (Fig. 3). However, our results show that H_2O_2 production was drastically decreased in *pad2-1* after OG elicitation or *P. brassicae* infection (Fig. 4; Supplemental Fig. S2). As there was no difference in the ability to degrade H_2O_2 between *pad2-1* and the wild type (Supplemental Fig. S1), this striking discrepancy highlights a central role of glutathione in the regulation of ROS production. As RbohD has been shown to be the main source of ROS detected after OG treatment (Galletti et al., 2008) or *P. brassicae* inoculation (Belhaj et al., 2009), these results indicate that *RbohD* gene expression is not sufficient to trigger enhanced NADPH oxidase activity but that post-translational modifications and upstream signaling events, like plasma membrane depolarization, are also needed (Gauthier et al., 2007, Jeworutzki et al., 2010). As NADPH oxidase activity is directly regulated by cytosolic Ca^{2+} partly released from internal pools such as the endoplasmic reticulum (Lecourieux et al., 2006; Vandelle et al., 2006), it is interesting that *S*-nitrosoglutathione influences cardiac reticulum Ca^{2+} release by activating the ryanodine receptor via *S*-nitrosylation (Sun et al., 2008). As *pad2-1* produces less NO and glutathione, one hypothesis would suggest that cytosolic Ca^{2+} variations might be impaired in *pad2-1*, thus explaining its impaired H_2O_2 production.

pad2-1 Is Impaired in Early Signaling Events Critical for HR Induction

Ion fluxes across membranes were shown to act upstream of PAMP-triggered early signaling events, including changes in plasma membrane potential, as well as H_2O_2 and NO synthesis (Garcia-Brugger et al., 2006; Gauthier et al., 2007; Jeworutzki et al., 2010). Our data show a strong decrease in plasma membrane depolarization in *pad2-1* cells responding to OG elicitation (Fig. 5). In the wild type, the use of the anionic channel inhibitor niflumic acid has shown that channel activity is involved in plasma membrane depolarization and acts upstream of ROS production during OG elicitation (Supplemental Fig. S3). In accordance with its lower plasma membrane depolarization, *pad2-1* also displayed reduced NO and H_2O_2 production in response to elicitor treatment or *P. brassicae* infection. These data are consistent with those of Belhaj et al. (2009), who found that the Arabidopsis *resistance to Phytophthora1* mutant, which is highly susceptible to *P. brassicae*, is also impaired in H_2O_2 production. More generally, the impairment of early signaling events observed in *pad2-1* might explain, at least partly, the strong reduction of HR in response to *P. brassicae* (Fig. 6). Indeed, plasma membrane depolarization and ROS and NO production have been reported to mediate pathogen- or PAMP-triggered defense gene expression and cell death (Wendehenne et al., 2002; Zago et al., 2006; Zaninotto et al., 2006; Hofius et al., 2007; Mur et al., 2008). In mammals, recent studies indicate that some channels could be regulated via *S*-glutathionylation (Yang et al., 2011). Thus, glutathione depletion could disturb ion fluxes across the plasma membrane, impairing its normal depolarization.

SA-Dependent Defense Responses, But Not the Indole Glucosinolate/Camalexin Pathway, Are Blocked at the Transcriptional Level in *pad2-1*

Glutathione has been shown to be important for inducing the SA-dependent defense pathway, notably by modifying the redox state of NPR1 (Després et al., 2003; Mou et al., 2003). Moreover, glutathione accumulation has been shown to coincide with SA production and the concomitant activation of the *PR-1* marker gene (Koornneef et al., 2008). Previous experiments have also demonstrated that *pad2-1* is impaired in the synthesis of SA and in *PR-1* gene expression (Roetschi et al., 2001; Parisy et al., 2007). Our results show that, in contrast to the wild type, *PR-1* gene expression remains very low during *P. brassicae* infection on *pad2-1* plants (Fig. 7). As *NPR1* gene expression was not affected in *pad2-1* (Fig. 7), it provides further evidence that redox regulation of the NPR1 protein is mandatory to trigger *PR-1* gene expression (Després et al., 2003; Mou et al., 2003; Pieterse and Van Loon, 2004). Using the glutathione-deficient *cad2-1* and *rax1-1* mutants, Ball et al. (2004) also showed that the content of glutathione influences the expression of other defense-related genes. However, redox regulation of NPR1 cannot fully explain how glutathione can modulate the level of SA. Because the ICS1 enzyme has been shown to participate in the biosynthesis of SA (Wildermuth et al., 2001), *ICS1* expression was followed in response to *P. brassicae*. Interestingly, we found that the normal up-regulation of *ICS1* gene expression after pathogen infection is totally abolished in *pad2-1* (Fig. 7), thus providing a possible explanation for the low SA levels observed in this mutant. As the two transcription factors SAR Deficient1 (SARD1) and CBP60g have been shown to be key regulators for *ICS1* expression induction via binding to its promoter (Zhang et al., 2010), further investigation will be needed to fully understand exactly how glutathione depletion and redox potential modifications affect SA biosynthesis.

Production of the secondary metabolites camalexin and indole glucosinolates is strongly affected in *pad2-1* in response to pathogens or insects (Glazebrook and Ausubel, 1994; Roetschi et al., 2001; Ferrari et al., 2003; van Wees et al., 2003; Parisy et al., 2007; Schlaeppi et al., 2008, 2010). Here, we show that these deficiencies are not caused by the down-regulation of genes encoding enzymes of the biosynthetic pathway, because *CYP79B2*, *CYP79B3*, *CYP81F2*, and *CYP71B15* are normally expressed in *pad2-1* in response to *P.*

brassicae (Supplemental Fig. S4). The camalexin and indole glucosinolate deficiencies are more likely to be caused by the lack of glutathione as a biosynthetic substrate. Glutathione was recently identified as the sulfur donor of camalexin and indole glucosinolate biosynthesis (Geu-Flores et al., 2009; Su et al., 2011). Furthermore, we cannot exclude that many heme-containing enzymes, such as cytochrome P450, could also be disturbed in their catalytic process by the distinct redox environment existing in *pad2-1* (Fig. 2). Indeed, it is interesting that the iron (III) protoporphyrin IX, important for P450 oxidoreductase activity, is maintained in the catalytic site by a thiol from a cysteinyl residue. This heme-Cys bond could probably be modified by the glutathione depletion, thus disturbing the normal electron transfer flow. In mammals, recent results have defined how thiol/disulfide redox switches control heme binding to regulate the activities of different enzymes (Ragsdale and Yi, 2011).

CONCLUSION

In summary, we report that the glutathione depletion in *pad2-1* is related to an alteration of GCL content associated with redox state modifications that disturb biological responses under normal and stress conditions. Our results highlight that glutathione modulates early signaling events (plasma membrane depolarization and ROS and NO production), governs oxidative stress-related processes (redox state and *GR1*, *GSTF6*, and *RbohD* gene expression), defense gene expression (*ICS1* and *PR-1*), and programmed cell death (HR) that normally enhance disease resistance. These deficiencies, in addition to the previously described deficiency in the accumulation of indole-derived secondary metabolites, are likely to contribute to the enhanced susceptibility of *pad2-1* to pathogens and pests.

MATERIALS AND METHODS

Cell Culture Conditions and Treatment

Arabidopsis (*Arabidopsis thaliana*) ecotype Col-0 wild-type and *pad2-1* cell suspensions were cultivated in Gamborg B5 medium (Duchefa; Gamborg et al., 1968) with 30 g L^{-1} Suc and 0.2 mg L^{-1} 1-naphthalene acetic acid (Duchefa) on a rotary shaker (120 rpm) at 24°C under continuous light (25 μmol m^{-2} s^{-1}). Cell suspension was routinely subcultured once per week. For elicitor treatment, cells were collected 1 d after subculturing, washed with M10 buffer (10 mM MES, 175 mM mannitol, 0.5 mM K_2SO_4, and 0.5 mM $CaCl_2$, pH 6.2), and resuspended at 0.1 g fresh weight of cells mL^{-1} M10 buffer. After 1 h of equilibration (125 rpm at 24°C), cells were treated with water or 0.5 g L^{-1} OG (Goëmar Laboratories), and measurements of plasma membrane depolarization or H_2O_2 production were performed.

Plant Growth Conditions and Treatment

Wild-type and *pad2-1*, *cad2-1*, and *rax1-1* mutant Arabidopsis plants were grown in Jiffy-7 peat pellets (Jiffy) in a controlled growth chamber under a 10/14-h day/night cycle at 20°C/18°C (70% relative humidity) with a light intensity of 175 μmol m^{-2} s^{-1} provided by fluorescent tubes.

The transformation of wild-type and *pad2-1* plants with GRX1-roGFP2 was done by floral dip, according to Clough and Bent (1998).

For elicitation, leaf discs (7 mm diameter) from 8-week-old plants were treated with water or 2.5 g L^{-1} OG in 50 mM Tris-HCl (pH 7.5) under vacuum conditions for 2 min and then collected at the indicated times. For NO production measurement, the NO scavenger carboxy-PTIO (0.5 mM; Sigma-Aldrich) and the fluorescent probe DAF-2DA (20 μM; Sigma-Aldrich) were added in the Tris buffer at the same time as OG. Precisely eight leaf discs from eight plants were used for each treatment. For GCL redox state analysis, 12 discs were cut and treated from three plants per kinetic point. For H_2O_2 detection, leaves were cut and infiltrated with 20 mM MES buffer (pH 6.2) containing 2.5 g L^{-1} OG, 10 units mL^{-1} peroxidase, and 1 g L^{-1} DAB (Sigma-Aldrich).

Pathogen Growth and Plant Inoculation

Phytophthora brassicae isolate D was routinely grown on 20% V8 agar medium (Campbell Foods) supplemented with 3.5 g L^{-1} $CaCO_3$ (pH 5) in a controlled chamber in the dark at 19°C.

For H_2O_2 detection and gene expression analysis, 4-week-old plants were inoculated by putting agar plugs of 8-d-old mycelium upside down on the leaf surface. Mycelium-free plugs were used for mock treatments. Twelve leaves from three plants per time point were used, and susceptibility was checked at 7 dpi by estimating symptom development as described previously (Parisy et al., 2007). For HR and susceptibility assays, plants were inoculated by spraying a suspension of zoospores at a concentration of 10^5 zoospores mL^{-1}. Inoculated plants were put under the same conditions as pathogen growth conditions at 100% relative humidity with a dark period for the first 14 h.

Measurement of Plasma Membrane Depolarization

Plasma membrane depolarization was monitored using the voltage-sensitive fluorescent probe $DiBAC_4(3)$ (Sigma-Aldrich; Konrad and Hedrich, 2008). After 1 h of equilibration, cells were incubated for 30 min with 10 μM $DiBAC_4(3)$ in M10 buffer in the dark. Then, 0.5 mL of cells was transferred onto 24-well plates (Costar) and treated with water or OG. $DiBAC_4(3)$ fluorescence was recorded at 1-min intervals using a fluorimeter (Fluoroskan Ascent Fluorometer [Labsystems]; $\lambda_{excitation}$ = 485 nm and $\lambda_{emission}$ = 535 nm) and expressed as relative fluorescence units. Cells were maintained under shaking during the course of the experiment.

H_2O_2 Production Measurement and Leaf Tissue Localization

In cell suspensions, H_2O_2 production was determined using the chemiluminescence of luminol. An aliquot of cells (250 μL) was added to 300 μL of H50 buffer (50 mM HEPES, 175 mM mannitol, 0.5 mM K_2SO_4, and 5 mM $CaCl_2$, pH 8.5) and 50 μL of 0.3 mM luminol. Chemiluminescence was measured with a luminometer (Lumat LB9507; Berthold). The content of H_2O_2 (nmol g^{-1} fresh weight of cells) was calculated using a calibration based on the addition of H_2O_2 to the aliquot of cells.

In plants, a modified procedure described by Thordal-Christensen et al. (1997) was applied. Leaves were vacuum infiltrated with 20 mM MES buffer (pH 6.2) containing 2.5 g L^{-1} OG, 1 g L^{-1} DAB, and 10 units mL^{-1} horseradish peroxidase, then washed with MES buffer. The same solution without OG was used as a control. Infiltrated leaves were incubated in the dark at room temperature for 1 to 8 h. Then, leaves were destained with a solution of glycerol:lactic acid:ethanol (1:1:3, v/v/v) at 85°C for 5 min. H_2O_2 production was visualized macroscopically as brown precipitates in plant tissues.

Measurement of H_2O_2 Half-Life, Total Peroxidase Activity, and Total Catalase Activity

H_2O_2 half-life and catalase activity were determined spectrophotometrically by measuring the absorbance of H_2O_2 at 240 nm, and peroxidase activity was determined by measuring the absorbance of oxidized guaiacol at 470 nm (for details, see Supplemental Protocol S1).

NO Production Measurement

Intracellular NO accumulation was determined using the specific fluorophore DAF-2DA (Sigma-Aldrich) as described by Besson-Bard et al. (2009).

Briefly, after infiltration and treatment with fluorophore, leaf discs were incubated for 1 h in the dark, washed three times with 50 mM Tris buffer, pH 7.5, to wash off excessive fluorophore, and transferred onto 96-well plates (Costar) containing 100 μL of the treatment solution. NO production was measured using a fluorimeter (Fluoroskan Ascent Fluorometer [Labsystems]; λ_{ex} = 485 nm and λ_{em} = 510 nm). Fluorescence was expressed as relative fluorescence units.

Protein Extraction and Western-Blot Analyses

Totals proteins were extracted from 12 leaf discs in 350 μL of extraction buffer (50 mM HEPES, 10 mM EGTA, 10 mM EDTA, 1 mM Na_3VO_4, 50 mM β-glycerolphosphate, 10 mM NaF, 5 mg L^{-1} leupeptin, 5 mg L^{-1} antipain, and 1 mM phenylmethylsulfonyl fluoride, pH 7.5) with or without 0.1 M DTT. After centrifugation (15 min, 10,000*g*), 15 μg of soluble proteins was treated with Laemmli buffer (4 min at 100°C) and subjected to 12% SDS-PAGE before transfer to nitrocellulose membranes (Hybond ECL; Amersham Biosciences) for western-blot analysis. GCL protein (At4g23100) was detected with an antibody raised against recombinant AtGCL (antibody provided by J. Jez, Donald Danforth Plant Science Center). Primary antibody detection was performed as described for the LumiGlo detection kit (Cell Signaling Technology) with a horseradish peroxidase-coupled secondary antibody (Sigma-Aldrich).

RNA Extraction and Real-Time Quantitative PCR Analysis

Total RNA was extracted using the total RNA isolation kit (Promega), and 1 μg of total RNA was reverse transcribed using the SuperScript III reverse transcriptase kit (Invitrogen). Real-time quantitative (q)PCR was performed using 2 μL of 80-fold diluted cDNA, ABsolute qPCR SYBR Green ROX mix (containing Taq polymerase, deoxyribonucleotide triphosphate, and SYBR Green dye; ABgene), and 500 nM primers (primer sequences are shown in Supplemental Table S1) in a 5-μL volume. Triplicate quantitative assays per biological experiment were performed by using the LightCycler480 detection system (Roche). The activation factor of gene expression was determined with the comparative cycle threshold (Ct) method (Livak and Schmittgen, 2001): $2^{-\Delta\Delta Ct}$; with $\Delta\Delta Ct = \Delta Ct(t = 24\ h) - \Delta Ct(t = 0)$ and $\Delta Ct = Ct(\text{target gene}) - Ct$ (reference gene) for both inoculated and mock samples. UBQ10 was used as the reference gene (Supplemental Table S1).

HR and Pathogen Development

The infected leaves were harvested at the appropriate time points and stained with an alcoholic lactophenol trypan blue solution (Keogh et al., 1980) by boiling for 1 min and keeping them overnight in the staining solution. Leaves were clarified in 70% (w/v) chloral hydrate solution in water. HR and pathogen structures were examined with a Leitz DM RB microscope (Leica).

Confocal Laser Scanning Microscopy Imaging and Ratiometric Analysis

Confocal laser scanning microscopy imaging and ratiometric analysis in wild-type and *pad2-1* plants expressing GRX1-roGFP2 were carried out as described by Schwarzländer et al. (2008). Briefly, the fluorescence of GRX1-roGFP2 was analyzed in leaf tissue of 7-d-old in vitro-grown seedlings. Images were taken with a 25× lens, in multitrack mode, with line switching and averaging of two frames. The probe was excited with a 405-nm laser in track 1 and with a 488-nm laser in track 2. GRX1-roGFP2 fluorescence was collected with a band-pass filter of 505 to 530 nm.

Ratiometric image analysis was done using a custom Matlab analysis suite as described by Schwarzländer et al. (2008).

Supplemental Data

The following materials are available in the online version of this article.

Supplemental Figure S1. Measurement of H_2O_2 half-life and total peroxidase and catalase activities in Col-0 and *pad2-1* plants.

Supplemental Figure S2. Intracellular NO production at 8 h after treatment with OG in Col-0 and *pad2-1* plants.

Supplemental Figure S3. Effect of the anionic channel inhibitor niflumic acid on OG-induced changes of plasma membrane potential and H_2O_2 production in Col-0 cell suspensions.

Supplemental Figure S4. Expression of genes involved in camalexin and glucosinolate biosynthesis in response to *P. brassicae* at 24 hpi.

Supplemental Table S1. Primers used for qPCR.

Supplemental Protocol S1. Measurement of H_2O_2 half-life, total peroxidase activity, and total catalase activity.

ACKNOWLEDGMENTS

We thank Agnès Klinguer and Delphine Desqué for excellent technical assistance and Joseph Jez for providing the anti-GCL antibody. We also thank François Bouteau for helpful discussion.

Received June 29, 2011; accepted October 15, 2011; published October 17, 2011.

LITERATURE CITED

Apel K, Hirt H (2004) Reactive oxygen species: metabolism, oxidative stress, and signal transduction. Annu Rev Plant Biol **55:** 373–399

Asai T, Tena G, Plotnikova J, Willmann MR, Chiu WL, Gomez-Gomez L, Boller T, Ausubel FM, Sheen J (2002) MAP kinase signalling cascade in Arabidopsis innate immunity. Nature **415:** 977–983

Ball L, Accotto GP, Bechtold U, Creissen G, Funck D, Jimenez A, Kular B, Leyland N, Mejia-Carranza J, Reynolds H, et al (2004) Evidence for a direct link between glutathione biosynthesis and stress defense gene expression in *Arabidopsis*. Plant Cell **16:** 2448–2462

Bednarek P, Pislewska-Bednarek M, Svatos A, Schneider B, Doubsky J, Mansurova M, Humphry M, Consonni C, Panstruga R, Sanchez-Vallet A, et al (2009) A glucosinolate metabolism pathway in living plant cells mediates broad-spectrum antifungal defense. Science **323:** 101–106

Belhaj K, Lin BQ, Mauch F (2009) The chloroplast protein RPH1 plays a role in the immune response of Arabidopsis to *Phytophthora brassicae*. Plant J **58:** 287–298

Besson-Bard A, Gravot A, Richaud P, Auroy P, Duc C, Gaymard F, Taconnat L, Renou JP, Pugin A, Wendehenne D (2009) Nitric oxide contributes to cadmium toxicity in Arabidopsis by promoting cadmium accumulation in roots and by up-regulating genes related to iron uptake. Plant Physiol **149:** 1302–1315

Besson-Bard A, Pugin A, Wendehenne D (2008) New insights into nitric oxide signaling in plants. Annu Rev Plant Biol **59:** 21–39

Bohman S, Staal J, Thomma BP, Wang ML, Dixelius C (2004) Characterisation of an Arabidopsis-*Leptosphaeria maculans* pathosystem: resistance partially requires camalexin biosynthesis and is independent of salicylic acid, ethylene and jasmonic acid signalling. Plant J **37:** 9–20

Boller T, Felix G (2009) A renaissance of elicitors: perception of microbe-associated molecular patterns and danger signals by pattern-recognition receptors. Annu Rev Plant Biol **60:** 379–406

Böttcher C, Westphal L, Schmotz C, Prade E, Scheel D, Glawischnig E (2009) The multifunctional enzyme CYP71B15 (PHYTOALEXIN DEFICIENT3) converts cysteine-indole-3-acetonitrile to camalexin in the indole-3-acetonitrile metabolic network of *Arabidopsis thaliana*. Plant Cell **21:** 1830–1845

Clough SJ, Bent AF (1998) Floral dip: a simplified method for *Agrobacterium*-mediated transformation of *Arabidopsis thaliana*. Plant J **16:** 735–743

Cobbett CS, May MJ, Howden R, Rolls B (1998) The glutathione-deficient, cadmium-sensitive mutant, *cad2-1*, of *Arabidopsis thaliana* is deficient in gamma-glutamylcysteine synthetase. Plant J **16:** 73–78

Delledonne M, Zeier J, Marocco A, Lamb C (2001) Signal interactions between nitric oxide and reactive oxygen intermediates in the plant hypersensitive disease resistance response. Proc Natl Acad Sci USA **98:** 13454–13459

Després C, Chubak C, Rochon A, Clark R, Bethune T, Desveaux D, Fobert PR (2003) The *Arabidopsis* NPR1 disease resistance protein is a novel cofactor that confers redox regulation of DNA binding activity to the basic domain/leucine zipper transcription factor TGA1. Plant Cell **15:** 2181–2191

Ferrari S, Plotnikova JM, De Lorenzo G, Ausubel FM (2003) Arabidopsis local resistance to *Botrytis cinerea* involves salicylic acid and camalexin and requires EDS4 and PAD2, but not SID2, EDS5 or PAD4. Plant J **35:** 193–205

Foissner I, Wendehenne D, Langebartels C, Durner J (2000) In vivo imaging of an elicitor-induced nitric oxide burst in tobacco. Plant J **23:** 817–824

Foyer CH, Bloom AJ, Queval G, Noctor G (2009) Photorespiratory metabolism: genes, mutants, energetics, and redox signaling. Annu Rev Plant Biol **60:** 455–484

Foyer CH, Noctor G (2011) Ascorbate and glutathione: the heart of the redox hub. Plant Physiol **155:** 2–18

Galletti R, Denoux C, Gambetta S, Dewdney J, Ausubel FM, De Lorenzo G, Ferrari S (2008) The AtrbohD-mediated oxidative burst elicited by oligogalacturonides in Arabidopsis is dispensable for the activation of defense responses effective against *Botrytis cinerea*. Plant Physiol **148:** 1695–1706

Gamborg OL, Miller RA, Ojima K (1968) Nutrient requirements of suspension cultures of soybean root cells. Exp Cell Res **50:** 151–158

Garcia-Brugger A, Lamotte O, Vandelle E, Bourque S, Lecourieux D, Poinssot B, Wendehenne D, Pugin A (2006) Early signaling events induced by elicitors of plant defenses. Mol Plant Microbe Interact **19:** 711–724

Gauthier A, Lamotte O, Reboutier D, Bouteau F, Pugin A, Wendehenne D (2007) Cryptogein-induced anion effluxes: electrophysiological properties and analysis of the mechanisms through which they contribute to the elicitor-triggered cell death. Plant Signal Behav **2:** 86–95

Geu-Flores F, Nielsen MT, Nafisi M, Møldrup ME, Olsen CE, Motawia MS, Halkier BA (2009) Glucosinolate engineering identifies a gamma-glutamyl peptidase. Nat Chem Biol **5:** 575–577

Glazebrook J (2005) Contrasting mechanisms of defense against biotrophic and necrotrophic pathogens. Annu Rev Phytopathol **43:** 205–227

Glazebrook J, Ausubel FM (1994) Isolation of phytoalexin-deficient mutants of *Arabidopsis thaliana* and characterization of their interactions with bacterial pathogens. Proc Natl Acad Sci USA **91:** 8955–8959

Glazebrook J, Rogers EE, Ausubel FM (1997) Use of Arabidopsis for genetic dissection of plant defense responses. Annu Rev Genet **31:** 547–569

Greenberg JT, Yao N (2004) The role and regulation of programmed cell death in plant-pathogen interactions. Cell Microbiol **6:** 201–211

Gromes R, Hothorn M, Lenherr ED, Rybin V, Scheffzek K, Rausch T (2008) The redox switch of gamma-glutamylcysteine ligase via a reversible monomer-dimer transition is a mechanism unique to plants. Plant J **54:** 1063–1075

Gutscher M, Pauleau AL, Marty L, Brach T, Wabnitz GH, Samstag Y, Meyer AJ, Dick TP (2008) Real-time imaging of the intracellular glutathione redox potential. Nat Methods **5:** 553–559

Halkier BA, Gershenzon J (2006) Biology and biochemistry of glucosinolates. Annu Rev Plant Biol **57:** 303–333

Hammerschmidt R (1999) Phytoalexins: what have we learned after 60 years? Annu Rev Phytopathol **37:** 285–306

Heath MC (2000) Hypersensitive response-related death. Plant Mol Biol **44:** 321–334

Hicks LM, Cahoon RE, Bonner ER, Rivard RS, Sheffield J, Jez JM (2007) Thiol-based regulation of redox-active glutamate-cysteine ligase from *Arabidopsis thaliana*. Plant Cell **19:** 2653–2661

Hofius D, Tsitsigiannis DI, Jones JDG, Mundy J (2007) Inducible cell death in plant immunity. Semin Cancer Biol **17:** 166–187

Hothorn M, Wachter A, Gromes R, Stuwe T, Rausch T, Scheffzek K (2006) Structural basis for the redox control of plant glutamate cysteine ligase. J Biol Chem **281:** 27557–27565

Jeworutzki E, Roelfsema MR, Anschütz U, Krol E, Elzenga JT, Felix G, Boller T, Hedrich R, Becker D (2010) Early signaling through the Arabidopsis pattern recognition receptors FLS2 and EFR involves Ca-associated opening of plasma membrane anion channels. Plant J **62:** 367–378

Jez JM, Cahoon RE, Chen SX (2004) *Arabidopsis thaliana* glutamate-cysteine ligase: functional properties, kinetic mechanism, and regulation of activity. J Biol Chem **279:** 33463–33470

Jones JDG, Dangl JL (2006) The plant immune system. Nature **444:** 323–329

Keogh RC, Deverall BJ, McLeod S (1980) Comparison of histological and physiological responses to *Phakopsora pachyrhizi* in resistant and susceptible soybean. Trans Br Mycol Soc **74:** 329–333

Konrad KR, Hedrich R (2008) The use of voltage-sensitive dyes to monitor signal-induced changes in membrane potential-ABA triggered membrane depolarization in guard cells. Plant J **55:** 161–173

Koornneef A, Leon-Reyes A, Ritsema T, Verhage A, Den Otter FC, Van Loon LC, Pieterse CM (2008) Kinetics of salicylate-mediated suppression of jasmonate signaling reveal a role for redox modulation. Plant Physiol **147:** 1358–1368

Lamotte O, Courtois C, Dobrowolska G, Besson A, Pugin A, Wendehenne D (2006) Mechanisms of nitric-oxide-induced increase of free cytosolic Ca^{2+} concentration in *Nicotiana plumbaginifolia* cells. Free Radic Biol Med **40:** 1369–1376

Lecourieux D, Ranjeva R, Pugin A (2006) Calcium in plant defence-signalling pathways. New Phytol **171:** 249–269

Levine A, Tenhaken R, Dixon R, Lamb C (1994) H_2O_2 from the oxidative burst orchestrates the plant hypersensitive disease resistance response. Cell **79:** 583–593

Livak KJ, Schmittgen TD (2001) Analysis of relative gene expression data using real-time quantitative PCR and the 2(-Delta Delta C(T)) method. Methods **25:** 402–408

Marrs KA (1996) The functions and regulation of glutathione S-transferases in plants. Annu Rev Plant Physiol Plant Mol Biol **47:** 127–158

Marty L, Siala W, Schwarzländer M, Fricker MD, Wirtz M, Sweetlove LJ, Meyer Y, Meyer AJ, Reichheld JP, Hell R (2009) The NADPH-dependent thioredoxin system constitutes a functional backup for cytosolic glutathione reductase in Arabidopsis. Proc Natl Acad Sci USA **106:** 9109–9114

Maughan SC, Pasternak M, Cairns N, Kiddle G, Brach T, Jarvis R, Haas F, Nieuwland J, Lim B, Müller C, et al (2010) Plant homologs of the *Plasmodium falciparum* chloroquine-resistance transporter, PfCRT, are required for glutathione homeostasis and stress responses. Proc Natl Acad Sci USA **107:** 2331–2336

May MJ, Vernoux T, Sánchez-Fernández R, Van Montagu M, Inzé D (1998) Evidence for posttranscriptional activation of gamma-glutamylcysteine synthetase during plant stress responses. Proc Natl Acad Sci USA **95:** 12049–12054

Meyer AJ, Brach T, Marty L, Kreye S, Rouhier N, Jacquot JP, Hell R (2007) Redox-sensitive GFP in *Arabidopsis thaliana* is a quantitative biosensor for the redox potential of the cellular glutathione redox buffer. Plant J **52:** 973–986

Mhamdi A, Hager J, Chaouch S, Queval G, Han Y, Taconnat L, Saindrenan P, Gouia H, Issakidis-Bourguet E, Renou JP, et al (2010) Arabidopsis GLUTATHIONE REDUCTASE1 plays a crucial role in leaf responses to intracellular hydrogen peroxide and in ensuring appropriate gene expression through both salicylic acid and jasmonic acid signaling pathways. Plant Physiol **153:** 1144–1160

Mittler R, Vanderauwera S, Gollery M, Van Breusegem F (2004) Reactive oxygen gene network of plants. Trends Plant Sci **9:** 490–498

Mou Z, Fan WH, Dong XN (2003) Inducers of plant systemic acquired resistance regulate NPR1 function through redox changes. Cell **113:** 935–944

Mullineaux PM, Rausch T (2005) Glutathione, photosynthesis and the redox regulation of stress-responsive gene expression. Photosynth Res **86:** 459–474

Mur LAJ, Kenton P, Lloyd AJ, Ougham H, Prats E (2008) The hypersensitive response: the centenary is upon us but how much do we know? J Exp Bot **59:** 501–520

Nawrath C, Métraux JP (1999) Salicylic acid induction-deficient mutants of *Arabidopsis* express PR-2 and PR-5 and accumulate high levels of camalexin after pathogen inoculation. Plant Cell **11:** 1393–1404

Noctor G (2006) Metabolic signalling in defence and stress: the central roles of soluble redox couples. Plant Cell Environ **29:** 409–425

Nutricati E, Miceli A, Blando F, De Bellis L (2006) Characterization of two Arabidopsis thaliana glutathione S-transferases. Plant Cell Rep **25:** 997–1005

Parisy V, Poinssot B, Owsianowski L, Buchala A, Glazebrook J, Mauch F (2007) Identification of PAD2 as a gamma-glutamylcysteine synthetase highlights the importance of glutathione in disease resistance of Arabidopsis. Plant J **49:** 159–172

Pfalz M, Vogel H, Kroymann J (2009) The gene controlling the indole glucosinolate modifier1 quantitative trait locus alters indole glucosinolate structures and aphid resistance in *Arabidopsis*. Plant Cell **21:** 985–999

Pieterse CM, Van Loon LC (2004) NPR1: the spider in the web of induced resistance signaling pathways. Curr Opin Plant Biol **7:** 456–464

Potters G, De Gara L, Asard H, Horemans N (2002) Ascorbate and glutathione: guardians of the cell cycle, partners in crime? Plant Physiol Biochem **40:** 537–548

Ragsdale SW, Yi L (2011) Thiol/disulfide redox switches in the regulation of heme binding to proteins. Antioxid Redox Signal **14:** 1039–1047

Reuber TL, Plotnikova JM, Dewdney J, Rogers EE, Wood W, Ausubel FM (1998) Correlation of defense gene induction defects with powdery mildew susceptibility in Arabidopsis enhanced disease susceptibility mutants. Plant J **16:** 473–485

Roetschi A, Si-Ammour A, Belbahri L, Mauch F, Mauch-Mani B (2001) Characterization of an Arabidopsis-Phytophthora pathosystem: resistance requires a functional PAD2 gene and is independent of salicylic acid, ethylene and jasmonic acid signalling. Plant J **28:** 293–305

Sagi M, Fluhr R (2006) Production of reactive oxygen species by plant NADPH oxidases. Plant Physiol **141:** 336–340

Schlaeppi K, Abou-Mansour E, Buchala A, Mauch F (2010) Disease resistance of Arabidopsis to *Phytophthora brassicae* is established by the sequential action of indole glucosinolates and camalexin. Plant J **62:** 840–851

Schlaeppi K, Bodenhausen N, Buchala A, Mauch F, Reymond P (2008) The glutathione-deficient mutant *pad2-1* accumulates lower amounts of glucosinolates and is more susceptible to the insect herbivore *Spodoptera littoralis*. Plant J **55:** 774–786

Schwarzländer M, Fricker MD, Müller C, Marty L, Brach T, Novak J, Sweetlove LJ, Hell R, Meyer AJ (2008) Confocal imaging of glutathione redox potential in living plant cells. J Microsc **231:** 299–316

Simon-Plas F, Elmayan T, Blein JP (2002) The plasma membrane oxidase NtrbohD is responsible for AOS production in elicited tobacco cells. Plant J **31:** 137–147

Su T, Xu J, Li Y, Lei L, Zhao L, Yang H, Feng J, Liu G, Ren D (2011) Glutathione-indole-3-acetonitrile is required for camalexin biosynthesis in *Arabidopsis thaliana*. Plant Cell **23:** 364–380

Sun J, Yamaguchi N, Xu L, Eu JP, Stamler JS, Meissner G (2008) Regulation of the cardiac muscle ryanodine receptor by O(2) tension and S-nitrosoglutathione. Biochemistry **47:** 13985–13990

Thordal-Christensen H, Zhang ZG, Wei YD, Collinge DB (1997) Subcellular localization of H_2O_2 in plants: H_2O_2 accumulation in papillae and hypersensitive response during the barley-powdery mildew interaction. Plant J **11:** 1187–1194

Torres MA, Dangl JL, Jones JDG (2002) Arabidopsis $gp91^{phox}$ homologues AtrbohD and AtrbohF are required for accumulation of reactive oxygen intermediates in the plant defense response. Proc Natl Acad Sci USA **99:** 517–522

Torres MA, Jones JDG, Dangl JL (2006) Reactive oxygen species signaling in response to pathogens. Plant Physiol **141:** 373–378

Tsuda K, Katagiri F (2010) Comparing signaling mechanisms engaged in pattern-triggered and effector-triggered immunity. Curr Opin Plant Biol **13:** 459–465

Vandelle E, Poinssot B, Wendehenne D, Bentéjac M, Alain P (2006) Integrated signaling network involving calcium, nitric oxide, and active oxygen species but not mitogen-activated protein kinases in BcPG1-elicited grapevine defenses. Mol Plant Microbe Interact **19:** 429–440

van Loon LC, Rep M, Pieterse CMJ (2006) Significance of inducible defense-related proteins in infected plants. Annu Rev Phytopathol **44:** 135–162

van Wees SCM, Chang HS, Zhu T, Glazebrook J (2003) Characterization of the early response of Arabidopsis to *Alternaria brassicicola* infection using expression profiling. Plant Physiol **132:** 606–617

Vernoux T, Wilson RC, Seeley KA, Reichheld JP, Muroy S, Brown S, Maughan SC, Cobbett CS, Van Montagu M, Inzé D, et al (2000) The *ROOT MERISTEMLESS1/CADMIUM SENSITIVE2* gene defines a glutathione-dependent pathway involved in initiation and maintenance of cell division during postembryonic root development. Plant Cell **12:** 97–110

Wendehenne D, Lamotte O, Frachisse JM, Barbier-Brygoo H, Pugin A (2002) Nitrate efflux is an essential component of the cryptogein signaling pathway leading to defense responses and hypersensitive cell death in tobacco. Plant Cell **14:** 1937–1951

Wildermuth MC, Dewdney J, Wu G, Ausubel FM (2001) Isochorismate synthase is required to synthesize salicylic acid for plant defence. Nature **414:** 562–565

Winterbourn CC (2008) Reconciling the chemistry and biology of reactive oxygen species. Nat Chem Biol **4:** 278–286

Yang Y, Shi W, Chen X, Cui N, Konduru AS, Shi Y, Trower TC, Zhang S, Jiang C (2011) Molecular basis and structural insight of vascular K(ATP) channel gating by S-glutathionylation. J Biol Chem **286:** 9298–9307

Zago E, Morsa S, Dat JF, Alard P, Ferrarini A, Inzé D, Delledonne M, Van Breusegem F (2006) Nitric oxide- and hydrogen peroxide-responsive gene regulation during cell death induction in tobacco. Plant Physiol **141:** 404–411

Zaninotto F, La Camera S, Polverari A, Delledonne M (2006) Cross talk between reactive nitrogen and oxygen species during the hypersensitive disease resistance response. Plant Physiol **141:** 379–383

Zhang Y, Xu S, Ding P, Wang D, Cheng YT, He J, Gao M, Xu F, Li Y, Zhu Z, et al (2010) Control of salicylic acid synthesis and systemic acquired resistance by two members of a plant-specific family of transcription factors. Proc Natl Acad Sci USA **107:** 18220–18225

Zhao Y, Hull AK, Gupta NR, Goss KA, Alonso J, Ecker JR, Normanly J, Chory J, Celenza JL (2002) Trp-dependent auxin biosynthesis in Arabidopsis: involvement of cytochrome P450s CYP79B2 and CYP79B3. Genes Dev **16:** 3100–3112